DISCRETE CELLULAR SCALES OF SOLAR CONVECTION

H. M. ANTIA and S. M. CHITRE

Tata Institute of Fundamental Research, Homi Bhabha Road, Bombay 400 005, India

(Received 16 January, 1992; in revised form 19 November, 1992)

Abstract. The theoretical power spectrum of velocity fields and flux fluctuations at the solar photosphere is calculated using a quasi-nonlinear framework of superposition of unstable convective eigenmodes excited in the solar convection zone. It is demonstrated that this power spectrum exhibits at least three distinct peaks corresponding to granulation, mesogranulation and supergranulation. The vertical velocity and the brightness fluctuation at the solar surface are found to be correlated. The theoretical framework can be adopted for application to other types of stars in order to predict the dominant length scales in the power spectrum of convection in these stars.

1. Introduction

One of the most striking properties of solar convective motions is the existence of distinct cellular scales observed at the surface of the Sun. Granulation, which has a characteristic scale-size of ≈ 2000 km and an average lifetime of 8–10 min, is visible largely through its brightness contrast; the typical vertical velocities associated with granulation are ≈ 1 km s^{-1}, while horizontal velocities are ≈ 2 km s^{-1} (Beckers and Canfield, 1976; Roudier *et al.*, 1991). Supergranulation with a cell-size of $\approx 30\,000$ km and lifetime of 1–2 days, is detected mainly through its horizontal flow pattern, and typically the horizontal velocities are of order 0.3–0.5 km s^{-1} (Hart, 1956, Simon and Leighton, 1964; Beckers, 1968). There is some uncertainty, however, about the vertical supergranular motion. Musman and Rust (1970) have reported vertical velocities in the range of 0.02–0.04 km s^{-1}; Worden and Simon (1976) observed a supergranular outflow of ≈ 0.05 km s^{-1}, while Giovanelli (1980) obtained an r.m.s. vertical velocity of ≤ 0.01 km s^{-1}. Recently, Wang and Zirin (1989) have measured an r.m.s. supergranular vertical velocity of ≈ 0.03 km s^{-1}. High-resolution observations of the Sun have revealed another scale of motion intermediate between granulation and supergranulation, namely, mesogranulation which has a mean size of ≈ 7000 km and lifetime of a few hours (November *et al.*, 1981). The existence of mesogranulation was originally deduced by November *et al.* (1981) from Dopplergrams of the vertical velocity field. But with the availability of techniques to measure proper motion of granules, the horizontal velocity fields at the solar surface could be observed directly (November and Simon, 1988) and the mesogranulation was confirmed by detection of ≈ 6000 km size structures in the horizontal flow field (Title *et al.*, 1986). Deubner (1989) studied the dynamics of mesogranulation to detect a distinct coherence of velocity and brightness fluctuations over the spatial scales $\approx 10\,000$ km. The r.m.s. horizontal velocities inferred from Deubner's power spectrum are ≈ 750 m s^{-1}, while the r.m.s. vertical motions are ≈ 300 m s^{-1}.

Solar Physics **145:** 227–239, 1993.

Besides these motions, giant cells which are comparable in size to the total thickness of the solar convection zone have also been inferred (Bumba, 1970; Howard, 1971).

An interesting question raised by these convective motions observed on the surface of the Sun is why the solar velocity power spectrum displays discrete spatial scales. Clearly, any reasonable theoretical model must not only explain the distinct peaks exhibited by the observed power spectrum of solar convection, but should also predict the preferred scales of convective motions on other stars which would, hopefully, become accessible to observations in the not too distant future. The cellular pattern detected in the solar photosphere must, in some way, be a manifestation of convective motions generated by instabilities in the superadiabatic sub-surface layers. Indeed, it is generally agreed that the solar granulation has a convective origin and is driven by the energy of hydrogen ionization in the strongly superadiabatic layers located several tens of kilometers below the photosphere (Simon and Weiss, 1968; Gough and Weiss, 1976). On the other hand, the mechanism that drives supergranulation is not altogether clear, although it has been proposed that supergranulation is a convective phenomenon attributed to energy from helium ionization at a depth of a few tens of thousand kilometers (Simon and Leighton, 1964; Simon and Weiss, 1968; Gough and Weiss, 1976). It is an interesting observational feature that the ratio of horizontal to vertical velocity of convective motions appears to be linearly dependent on the spatial scale; thus the ratio is of order 1 for granules, ≈ 2.6 for mesogranules and ≈ 20 for supergranules (Hill, Deubner, and Isaak, 1991).

In an attempt to understand the granular scale, Böhm (1963) calculated the growth rates of linear convective modes in an equilibrium solar convection zone model constructed with the mixing-length formalism. The resulting growth rates showed a monotonic increase with decreasing wavelength well past the observed cut-off; this could be attributed to neglect of the turbulent thermal conductivity in Böhm's analysis. Evidently, most of the flux in the convection zone is carried by convective processes and furthermore, the radiative conductivity is negligible compared to the turbulent heat conductivity in this zone. It is therefore, expected that the turbulent processes will have significant influence on the manner in which the thermal flux in the solar convection zone is transported. This prompted Antia, Chitre, and Pandey (1981) to extend Böhm's work and to investigate the stability of linear convective modes in the solar convection zone by incorporating the mechanical and thermal effects of turbulence through the eddy transport coefficients. The underlying assumption is that both the coefficients of turbulent thermal conductivity and turbulent viscosity can be satisfactorily constructed with the help of the mean convective velocity and the local mixing length.

It was demonstrated by Antia, Chitre, and Pandey (1981) that the character of convective eigenmodes is very significantly influenced by the inclusion of turbulent transport coefficients. When the background solar convection zone model was perturbed, the resulting most rapidly growing fundamental eigenmode and the first subharmonic were found to be in reasonable accord with the observed features of granulation and supergranulation, respectively.

The main thrust of the present work is to study linear stability characteristics of

convective eigenmodes with a view to derive the power spectrum of the solar velocity field using the linear superposition technique for reproducing the model convective flux. It is then demonstrated that the power spectrum at the surface of the Sun, indeed, exhibits the distinct peaks corresponding to granulation, mesogranulation and supergranulation. This may be compared with the observed power in these features of solar convection. The theoretical framework is extended for application to other types of stars (e.g., α Cen A (G2 V) and Arcturus (K1 III)) in order to predict the dominant length scales in the power spectrum of convection on these stars.

2. Theoretical Model and Governing Equations

A realistic solar convection zone model is constructed using a non-local mixing length prescription adopted by Shaviv and Chitre (1968). Here the mean convective velocity is calculated by including the aerodynamic drag experienced by moving elements. Thus, a descending element that is distorted because of the eddies generated around it during its motion in the midst of ascending elements, suffers resistance, and this manifests as a drag which is determined mainly by the energy dissipated in the wake. When this aerodynamic drag is incorporated in the motion, the non-locality in the velocity profile is simulated by the equation (Antia, Chitre, and Narasimha, 1984):

$$\frac{\mathrm{d}W^2}{\mathrm{d}r} = \frac{\beta g Q L}{H_p} (\nabla - \nabla_{\mathrm{ad}}) - \frac{D W^2}{L} \,. \tag{1}$$

Here β is a parameter of order unity and $D = 4C_D$, where C_D is the aerodynamic drag coefficient, L is the mixing length, W the mean velocity of convective elements, H_p the local pressure scale height, $Q = -(\partial \ln \rho / \partial \ln T)_P$, $\nabla = (\mathrm{d} \ln T / \mathrm{d} \ln P)$, $\nabla_{\mathrm{ad}} = (\partial \ln T / \partial \ln P)_s$, and r is the radial distance. The standard stellar structure equations with the mixing-length approximation are integrated using Equation (1) for the velocity (cf. Antia, Chitre, and Narasimha, 1984). Since the convective modes are trapped in the convection zone it is sufficient to consider only the outer layers of the Sun. We have used a solar envelope model which extends up to a depth of 250 000 km. In the atmosphere above the optical depth $\tau = 1$ we use a model based on an empirical $(T - \tau)$ relation given by Vernazza, Avrett, and Loeser (1976). The outer boundary of the model is chosen to be around the temperature minimum. The solar composition is assumed to be ($X = 0.732$, $Y = 0.250$, $Z = 0.018$). The opacity tables of Cox and Tabor (1976) have been used, along with the molecular opacities by Alexander (1975) at low temperatures.

This equilibrium solar model is perturbed to calculate the linear convective eigenmodes by incorporating the eddy transport coefficients. For studying the linear stability, we adopt the usual hydrodynamical equations governing the conservation of mass, momentum and energy as applicable to a viscous, thermally-conducting fluid layer:

mass conservation:

$$\frac{\partial \rho}{\partial t} + \nabla \cdot (\rho \mathbf{v}) = 0 \,, \tag{2}$$

momentum conservation:

$$\rho \frac{\partial \mathbf{v}}{\partial t} + \rho(\mathbf{v}\cdot\nabla)\mathbf{v} = \rho\mathbf{g} - \nabla P - \tfrac{2}{3}\mu_t\nabla(\nabla\cdot\mathbf{v}) - \tfrac{2}{3}(\nabla\cdot\mathbf{v})\nabla\mu_t + \\ + \nabla\cdot[\mu_t(\nabla\mathbf{v} + \mathbf{v}\nabla)], \tag{3}$$

energy conservation:

$$\rho T\left(\frac{\partial s}{\partial t} + \mathbf{v}\cdot\nabla s\right) = -\nabla\cdot(\mathbf{F}^R + \mathbf{F}^C) + \Phi, \tag{4}$$

where the rate of viscous dissipation

$$\Phi = \tfrac{1}{2}\mu_t(\nabla\mathbf{v} + \mathbf{v}\nabla)\cdot(\nabla\mathbf{v} + \mathbf{v}\nabla) - \tfrac{2}{3}\mu_t(\nabla\cdot\mathbf{v})^2. \tag{5}$$

Here we have adopted the usual notation with s as the specific entropy, P the thermodynamic pressure, F^R the radiative flux, and F^C the convective flux. The turbulent viscosity $\mu_t = \sigma_t\alpha\rho WL$, where σ_t is the turbulent Prandtl number and α is another parameter of order unity. The mixing-length L is chosen to be the distance from the nearest boundary of the convection zone. Apart from the gas pressure, we have also included a contribution due to the turbulent pressure $P_t = C_\rho W^2$, where C is a constant. Using the Eddington approximation, the radiative flux $\mathbf{F}^R$ is given by (Unno and Spiegel, 1966)

$$\mathbf{F}^R = -\frac{4}{3\kappa\rho}\nabla J, \qquad J = \sigma T^4 - \frac{\nabla\cdot\mathbf{F}^R}{4\kappa\rho}, \tag{6}$$

where κ is the mean Rosseland opacity, J is the intensity of radiation, and σ the Stefan–Boltzmann constant.

The convective flux in the mixing length formalism is given by

$$\mathbf{F}^C = -\alpha\rho C_p WL\left(\nabla T - \nabla_{\mathrm{ad}}\frac{T}{P}\nabla P\right). \tag{7}$$

For the purpose of the present calculations, we choose the values $\alpha = 0.25$, $\beta = 0.25$, $L = \min(z + 459\ \mathrm{km}, 215\,000 - z\ \mathrm{km})$, where z is the depth measured from $\tau = 1$ level, $D = 0.1$ to 1, while the turbulent Prandtl number σ_t is chosen to take values between $\frac{2}{3}$ and $\frac{3}{2}$.

The governing equations are linearized to obtain a set of nine first-order differential equations for the perturbed quantities in the convection zone, while the bounding overlying atmosphere as well as the underlying radiative interior are assumed to be inviscid. The set of equations along with the required connection and boundary conditions, as given by Antia, Chitre, and Narasimha (1984), constitute a generalized eigenvalue problem. The real eigenvalues and the associated eigenfunctions are determined numerically, adopting a finite-difference method (Antia, 1979) for a specified value of

the horizontal harmonic number l. For each value of l there is a sequence of modes which is characterized by the number of nodes in the eigenfunction. The fundamental mode with the largest eigenvalue is referred to as the $C1$ mode, while the first subharmonic is referred to as the $C2$ mode. Here the suffixes 1 and 2 refer to the radial order n (cf. Equation (8)). In most cases considered here only the $C1$ mode turns out to be unstable, while in some cases the $C2$ mode is also unstable. Thus, we only consider the $C1$ and (in some cases) $C2$ modes. The higher subharmonics which are stable are not included in this study.

3. Modal Analysis and Theoretical Power Spectrum

An interesting question addressed by Hart (1973) was whether stellar convection zone models constructed using the framework of the mixing-length theory are consistent with models incorporating convection dynamics. It was convincingly shown by Hart (1973) and Bogart, Gierasch, and Macauslan (1980) that no linear superposition of adiabatic, inviscid eigenmodes could even remotely reproduce the model convective flux profile of the solar convective envelope. This was a direct consequence of all the convective modes having a sharp peak in the strongly superadiabatic region just below the photosphere. It was demonstrated by Narasimha and Antia (1982) that the convection zone models constructed by adopting the mixing length prescription can indeed be made consistent with models incorporating convection dynamics, provided the mechanical and thermal effects of turbulent convection are included in the stability analysis through the turbulent transport coefficients. In fact, Narasimha and Antia (1982) found that with the inclusion of turbulent thermal conductivity, the eigenfunctions no longer peaked only in the subsurface superadiabatic region, but rather they were spread over the entire convection zone. The linear eigenfunctions with large values of harmonic number, l, peak near the surface, while those corresponding to small l peak near the base of the convection zone.

The energy flux, $F_{ln}(r)$ carried by a given eigenmode with angular harmonic number l and radial order n may be calculated using the expression

$$F_{ln}(r) = \rho_0 v_r (T_0 s_1 + P_1/\rho_0)\,, \tag{8}$$

where ρ_0 and T_0 are, respectively, the density and temperature in the equilibrium solar model, while v_r, P_1, and s_1 are the perturbations in vertical velocity, pressure, and specific entropy, respectively. The perturbed quantities are computed from the eigenfunction corresponding to the relevant eigenmode. In order to fix the normalization, the multiplicative constant in the eigenfunctions is so chosen that the maximum of the convective flux, $F_{ln}(r)$, over the entire convection zone equals the total solar flux at that depth. The superposition of these eigenmodes to match the convective flux profile computed in the mixing length framework at various depths may be used to determine the amplitudes of the eigenmodes by writing

$$\sum_{l,n} a_{ln}^2 F_{ln}(r) = F_0^C(r)\,, \tag{9}$$

where $F_0^C(r)$ is the equilibrium convective flux profile calculated adopting the mixing-length prescription, and a_{ln} is the amplitude of the corresponding convective eigenmode. It is then demonstrably possible to find a linear superposition of statistically independent, unstable convective modes which can reproduce the model convective flux reasonably well throughout the solar convection zone. Using a few representative values of l we can obtain a least-squares solution of this equation to determine the amplitudes a_{ln} of individual eigenmodes. The technique of superposing these linear eigenmodes to match the convective flux profile obtained with the mixing-length prescription can thus be effectively used to determine the amplitudes of various eigenmodes. The linear stability analysis would evidently not have yielded the amplitude of a given mode, but the present approach, which in some sense simulates the nonlinear effects through the eddy transport coefficients, is able to yield the amplitudes when the convective flux constructed for individual eigenmodes peaking at different depths is matched with the model convective flux. This, in our view, is a quasi-nonlinear approach to the problem of convection dynamics, which helps us to fix the amplitudes of convective modes within the framework of the linearized theory. Its effectiveness can only be tested by comparing the results with elaborate, three-dimensional, numerical simulation of hydrodynamical flows (cf. Stein and Nordlund, 1989; Chan and Sofia, 1986). The main inquiry we must now address is whether such a quasi-nonlinear approach can reasonably reproduce the scales detected on the solar surface and, more importantly, predict the corresponding features on other stars.

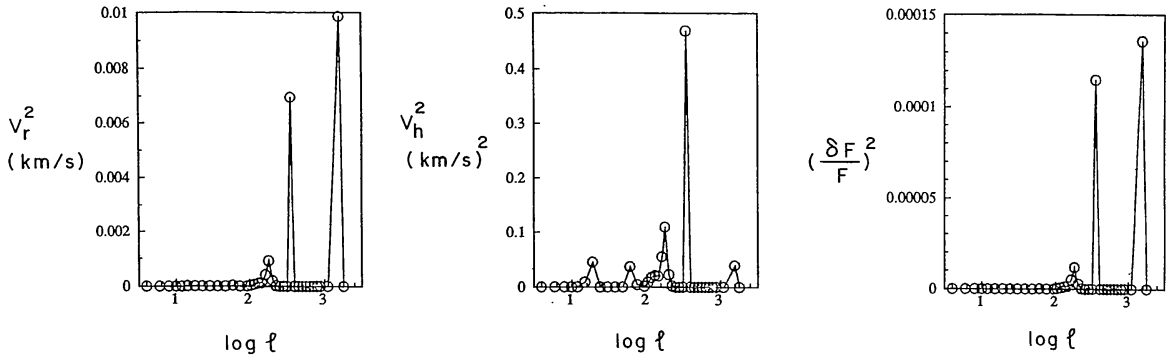

Fig. 1. Power spectrum of vertical velocity (V_r), horizontal velocity (V_h), and flux perturbation ($\delta F/F$) for a solar model with $C = 0.5$, $D = 0.5$, and with turbulent Prandtl number $\sigma_t = 0.85$.

We have displayed in Figure 1 the horizontal and radial velocity components at optical depth $\tau = 0.4$, as a function of the logarithm of the horizontal harmonic number l, for the solar case. For the purpose of obtaining the power per unit mode as a function of l we select a set $\{l_1, l_2, \ldots, l_N\}$ $(l_1 < l_2 < \cdots < l_N)$ of representative values of l spanning the entire range of unstable convective modes. The amplitudes of the modes in a linear superposition are then obtained as described above and these amplitudes are then converted to power per mode by assuming that each l_i represents a typical mode in the interval $((l_{i-1} + l_i)/2, (l_i + l_{i+1})/2)$. This would essentially amount to the calculat-

ed amplitude a_{l_i} being divided by $(l_{i+1} - l_{i-1})/2$ in order to obtain the corresponding value of power per mode. The points actually used to obtain the curve are indicated explicitly in the figures. The total power due to modes in a given interval of l can be determined by summing the power in all modes in the required interval. It should be noted that the final result will naturally depend on the choice of $\{l_i\}$ used to obtain the least-squares solution. We have repeated the calculations with different choices for $\{l_i\}$ to find that the power spectrum does, in fact, depend to some extent on this choice, but the total power in a given range of l values turns out to be not very sensitive. The general shape of the power spectrum is independent of the choice, but the height and exact position of the peaks do depend on the choice of $\{l_i\}$. Hence, it is more meaningful to compare the total power in different peaks with observations. Further, since the amplitudes are determined by a least-squares solution, it is not possible to accurately determine the amplitudes of those modes which have low power. Consequently, we have shown the power spectrum in Figures 1, 2, and 3 plotted on a logarithmic scale for l only.

We notice from Figure 1 that the most striking feature of the velocity power spectrum is the presence of three distinct peaks at $l \approx 1500$, $l \approx 350$, and $l \approx 180$, with possible peaks around $l \approx 20$ and 60. The existence of preferred scale-sizes on the solar surface is thus clearly indicated by the theoretical power spectrum of solar convection. The theoretically computed maximal length scales, $\lambda = 2\pi R_\odot/\sqrt{l(l+1)}$ corresponding to the three peaks are around 2800, 12 000, and 24 000 km, in reasonable accord with the observed length scales associated respectively with granulation, mesogranulation and supergranulation. It is tempting to identify the smaller peaks at $l \approx 19$ and 60, which are noticeable only in the power spectrum for the horizontal component of velocity, with global convection (Howard and LaBonte, 1980; Schröter, 1985). This power spectrum may be compared with observations of Chou *et al.* (1991) and Beckers (1981). Ginet and Simon (1992) have further analyzed and interpreted the observations of Chou *et al.* (1991) to report an r.m.s. horizontal velocity of ≈ 0.23 km s^{-1} for mesogranulation. Note that in the present work the power per mode is calculated with respect to the harmonic number l, while in the observational results of Chou *et al.* (1991) the power is expressed in terms of the horizontal wave number (rad Mm^{-1}). We remark that there are no unstable convective modes beyond $l = 2000$ for our solar envelope model. From this we infer that cellular structures of sizes exceeding ≈ 2000 km are of convective origin, and they carry most of the convective flux, while the smaller scale eddies are produced via the turbulent energy cascade process (cf. Roudier *et al.*, 1991).

It is interesting to compute the associated fluctuation in the flux $\delta F/F$, and these results are also shown in Figure 1. Again, the power spectrum of flux variation exhibits peaks at the discrete scales corresponding to granulation, mesogranulation and supergranulation. The flux variation is evidently dominated by a granular component whose contribution is nearly a factor of three larger than that of the mesogranulation. We should like to emphasize that in our analysis the flux perturbation appears to be directly correlated with the vertical component of velocity at the photospheric level.

It is straightforward to estimate the total power in different scales by calculating the

TABLE I

Power spectrum of stellar convection

Model	Mode	l_{max}	Length scale (km)	Time scale (hr)	Total power		
					V_r (km s^{-1})	V_h (km s^{-1})	$\delta F/F$
Sun (A)	$C1$	1570	2.8×10^3	0.6	1.8×10^0	3.68	2.2×10^{-1}
$C = 0.5$, $D = 0.5$	$C1$	356	1.2×10^4	5.1	5.5×10^{-1}	4.53	7.0×10^{-2}
$\sigma_t = 0.85$	$C1$	182	2.4×10^4	137	1.8×10^{-1}	2.05	2.0×10^{-2}
	$C1$	60	7.2×10^4	232	2.2×10^{-2}	0.75	1.8×10^{-3}
	$C1$	19	2.2×10^5	806	2.8×10^{-3}	0.48	2.5×10^{-5}
Sun (B)	$C1$	1960	2.2×10^3	0.5	1.9×10^0	3.47	1.8×10^{-1}
$C = 0.01$, $D = 0.1$	$C1$	356	1.2×10^4	1.7	3.7×10^{-1}	4.27	1.6×10^{-2}
$\sigma_t = 1.00$	$C1$	164	2.7×10^4	11.5	9.5×10^{-2}	2.09	3.4×10^{-3}
	$C1$	30	1.4×10^5	83	4.2×10^{-3}	0.48	1.2×10^{-3}
	$C1$	10	4.2×10^5	183	7.1×10^{-4}	0.30	4.8×10^{-4}
Sun (C)	$C1$	1110	3.9×10^3	0.7	1.2×10^0	4.10	8.7×10^{-2}
$C = 0.01$, $D = 0.1$	$C1$	320	1.4×10^4	2.8	2.9×10^{-1}	3.35	1.6×10^{-3}
$\sigma_t = 1.50$	$C1$	146	3.0×10^4	48	6.2×10^{-2}	1.25	4.1×10^{-3}
	$C1$	38	1.1×10^5	204	5.8×10^{-3}	0.43	1.4×10^{-3}
	$C1$	12	3.5×10^5	202	8.7×10^{-4}	0.29	6.1×10^{-4}
α Cen A	$C1$	1110	4.8×10^3	1	1.6×10^0	4.05	1.6×10^{-1}
$C = 0.01$, $D = 0.1$	$C1$	285	1.9×10^4	5	4.9×10^{-1}	4.01	3.5×10^{-2}
$\sigma_t = 1.50$	$C1$	132	4.1×10^4	93	1.6×10^{-1}	1.76	7.8×10^{-3}
	$C1$	38	1.4×10^5	1070	2.4×10^{-2}	0.65	3.2×10^{-4}
Arcturus	$C1$	50	1.5×10^6	76	1.7×10^0	4.41	1.3×10^{-1}
$C = 1$, $D = 1$	$C1$	8	9.0×10^6	5500	2.6×10^{-1}	5.11	4.5×10^{-2}
$\sigma_t = 0.75$	$C2$	4	1.7×10^7	7500	3.6×10^0	4.47	1.5×10^{-1}

area under the corresponding peaks. The results are displayed in Table I. It may be noted that in some cases different quantities (e.g., V_r and V_h) have peaks at slightly different l values. In such cases, one of these values which appears to be more dominant is listed in the third column of Table I. In the linear approximation, the time-scale corresponding to each of these modes may be expected to be of the order of the e-folding time of the eigenmode. This estimate is also listed in the table. We recall that the observed r.m.s. values of the vertical (V_r) and horizontal (V_h) velocities are reported to be $\lesssim 1$ km s^{-1} and $\lesssim 2$ km s^{-1} for granulation; ≈ 0.3 km s^{-1} and ≈ 0.75 km s^{-1} for mesogranulation; ≈ 0.05 km s^{-1} and ≈ 0.5 km s^{-1} for supergranulation. These numbers may be compared with the theoretical values in Table I. Observationally, it is found that the ratio of vertical to horizontal velocities decreases linearly with cell size. It is interesting that a similar trend can be seen in the theoretical values listed in the table.

With a view to study the sensitivity of the power spectrum to various mixing length parameters, several different combinations were attempted. In all cases, the three peaks corresponding to granulation, mesogranulation and supergranulation dominate the spectrum, although their position and strength may vary a little. Table I summarizes the

relevant properties of the power spectrum for a few selected models. In particular, it is found that even if the turbulent pressure is effectively suppressed, by reducing the parameter $C = P_t/(\rho W^2)$ to 0.01, the three peaks are still found to survive. It may be noted (cf. Antia, Chitre, and Pandey, 1981) that for this model the plot of growth rate of the fundamental mode as a function of l has only one peak corresponding to granulation. The power spectrum for the solar model with $C = 0.01$ and $D = 0.1$ is shown in Figure 2. It can be seen that the power spectrum exhibits three peaks at length scales roughly corresponding to those of granulation, mesogranulation and supergranulation, together with the peaks at the larger scales corresponding to global convection. We recall that Antia, Chitre, and Narasimha (1983) had stressed the importance of turbulent pressure in producing the double peak in the plot of growth rate for the $C1$-mode. From the present work it appears that, irrespective of the number of peaks in the growth rate vs l plot, the power spectrum always displays three dominant peaks, and this turns out to be the robust feature of the theoretically computed power spectrum of solar convection. Apart from these three peaks there are two smaller peaks at large length scales in the power spectrum for horizontal velocity. From Table I it is clear that the position of these peaks depends rather sensitively on the mixing length parameters used to construct an equilibrium solar model.

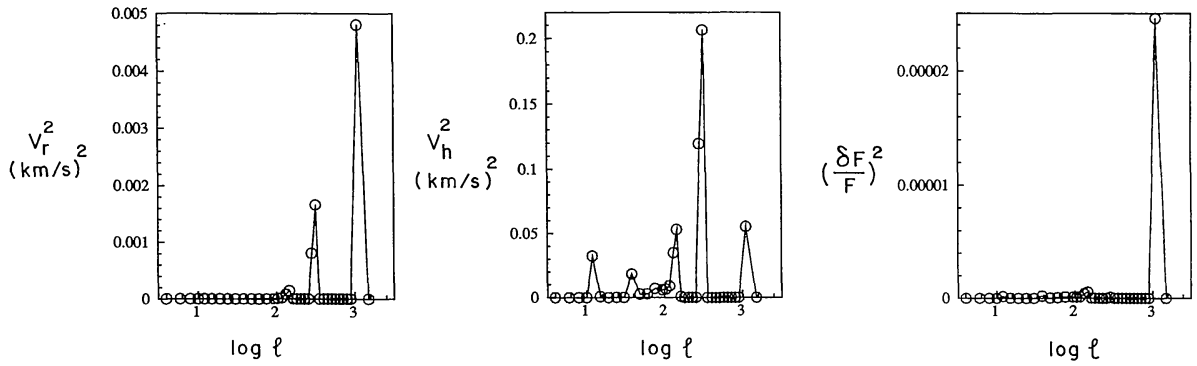

Fig. 2. Power spectrum of vertical velocity (V_r), horizontal velocity (V_h), and flux perturbation ($\delta F/F$) for a solar model with $C = 0.01$, $D = 0.1$, and with turbulent Prandtl number $\sigma_t = 1.5$.

From Table I it is clear that the values for horizontal velocity components for different scales turn out to be higher by a factor of two to five as compared to the corresponding observed values. This discrepancy could be due to inadequate treatment of radiative and viscous dissipation in the atmosphere. It may be stressed that the amplitudes of these modes are determined by eigenfunctions within the convection zone, while the power spectrum is computed at the solar photosphere around $\tau = 0.4$. Thus, even if the eigenfunctions are modified in the atmosphere, the amplitudes a_{ln} as determined from the least-square fit, may not be appreciably affected, since these values are essentially determined by the flux profile inside the convection zone. In particular, a departure from radiative equilibrium may affect the eigenfunction in the atmosphere significantly (Christensen-Dalsgaard and Frandsen, 1983). Apart from this, increasing the viscosity

can also affect the velocity. For example, the models (B) and (C) in Table I differ only in the turbulent Prandtl number σ_t, and it is clear that increasing the viscosity reduces the velocity in the mesogranular and supergranular peaks significantly. It is not desirable to increase σ_t beyond this value, since in that case some of the eigenmodes in intermediate range of l values become stable, and it becomes difficult to construct a linear superposition of modes to reproduce the convective flux. Nevertheless, it is possible to increase the viscosity selectively in the atmosphere to reduce the velocity amplitudes at the photosphere without significantly affecting the stability characteristic of the convective modes. Thus, if the viscosity is increased by a factor of three in the atmosphere, then the horizontal velocity contribution from the three peaks are 3.74, 2.42, and 0.76 km s^{-1}, while the vertical velocity is 0.69, 0.11, and 0.014 km s^{-1}.

Table I gives only the power at the photospheric level. The total kinetic energy associated with the mode can be calculated by integrating the eigenfunctions across the entire thickness of the convection zone. Since the convective modes with small l penetrate rather deep into the convection zone, the effective mass associated with them is much larger and this gives much higher kinetic energy in eddies with larger scales. On the other hand, the modes associated with granulation ($l \approx 1500$) do not penetrate far below the photosphere and even though the velocity may be large, the associated mass is considerably smaller and the total kinetic energy is several orders of magnitude lower than that for low l modes. This is perhaps suggestive of the direct energy cascade with the kinetic energy of granulation being derived from the larger scales of convective motion (Zahn, 1987).

This study can be extended even to other stars and we have considered two stars for the sake of illustration: the Sun-like star α Cen A and the red giant Arcturus. The results for α Cen A (G2 V) and Arcturus (K III) are summarized in Table I. For this purpose, we use the stellar envelope models constructed by Antia and Pandey (1989). Following the solar case we use $C = 0.01$, $D = 0.1$, and $\sigma_t = 1.5$ for α Cen A. The power spectrum for α Cen A (Figure 3) is similar to that of the Sun, except for the fact that the corresponding length scales tend to be slightly larger. Once again, the fourth peak at small values of l is noticeable only in the horizontal velocity component V_h. For

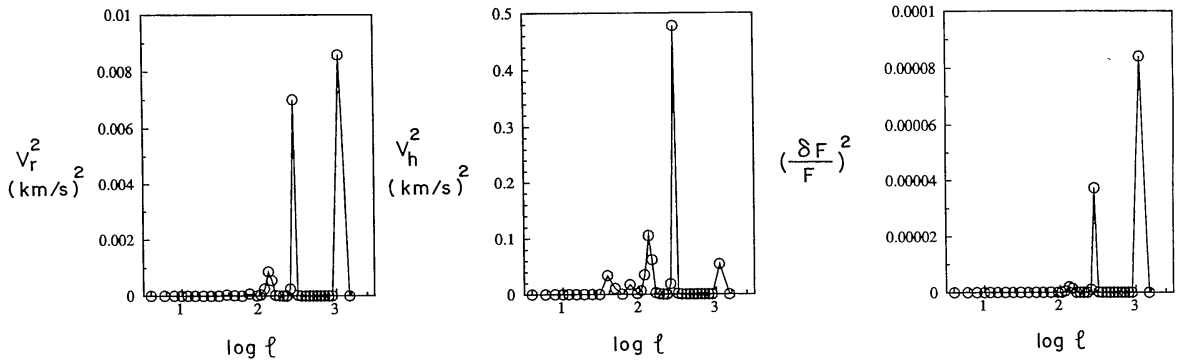

Fig. 3. Power spectrum of vertical velocity (V_r), horizontal velocity (V_h), and flux perturbation ($\delta F/F$) for a model of α Cen A with $C = 0.01$, $D = 0.1$, and with turbulent Prandtl number $\sigma_t = 1.5$.

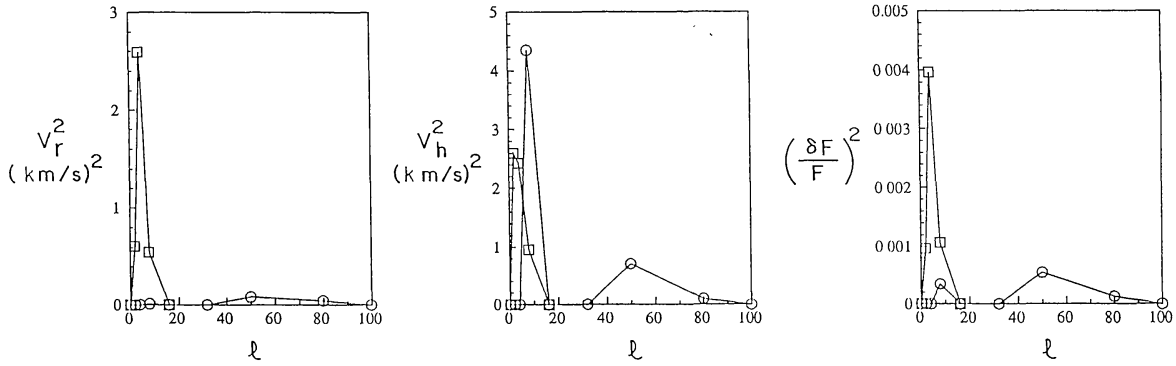

Fig. 4. Power spectrum of vertical velocity (V_r), horizontal velocity (V_h), and flux perturbation ($\delta F/F$) for a model of Arcturus with $C = 1$, $D = 1$, and with turbulent Prandtl number $\sigma_t = 0.75$.

Arcturus (Figure 4) the length scales as well as time scales are much larger and the $C2$-mode appears to dominate the power spectrum.

4. Conclusions

The most important conclusion from our study is that for a wide range of mixing length parameters covering most reasonable solar convection zone models, we find that the theoretical power spectrum of the solar convective velocity field has at least three distinct peaks at length scales corresponding to granulation, mesogranulation and supergranulation. The power spectrum for the horizontal component of velocity shows two more peaks possibly corresponding to scales of global convection. In particular, a scale around 100 000 km seems to be indicated. Furthermore, the power spectrum of flux-variation also exhibits peaks at these discrete scales. It is, of course, possible to shift the peaks somewhat with different sets of parameters or by changing the outer boundary conditions.

In the present calculation the contribution of small scales of turbulence is included by constructing eddy diffusivity coefficients, with the magnitude of transport coefficients taken to be proportional to WL, where both W and L vary with depth – thus the mixing-length L has values of the order of a few hundred kilometers near the surface but is of order of a hundred thousand kilometers in the middle of the convection zone. In this manner, while evaluating the turbulent heat conductivity and the turbulent viscosity, we have included contributions due to smaller scale eddies, but the larger scales are, of course, neglected.

An interesting feature is the size of the dominant convective elements on α Cen A and Arcturus: the dominant $C1$ modes are similar to solar granulation, mesogranulation and supergranulation on α Cen A, but in the case of Arcturus, the unstable convective modes with small values of l (~ 4–50) dominate the brightness fluctuations. We, therefore, expect only a limited number of such large granules to cover the surface of Arcturus at any given time. The granules can cause significant variations in the stellar intensity over time scales of the order of three days, which is within the characteristic time of irregular

variation of light observed in red giants. Interestingly, even with only a few tens of unstable convective modes it is demonstrably possible to construct a linear superposition of these modes, which can reasonably reproduce the model convective flux profile. The quasi-nonlinear technique is thus evidently applicable both for Sun-like stars and late-type giants with large convective envelopes. Of course, it still remains to be seen whether the results predicted for these stars are verified by actual observations.

Acknowledgement

The authors are grateful to the referee for his stimulating comments, which have led to a considerable improvement in the manuscript.

References

Alexander, D. R.: 1975, *Astrophys. J. Suppl.* **29**, 363.
Antia, H. M.: 1979, *J. Comp. Phys.* **30**, 283.
Antia, H. M. and Pandey, S. K.: 1989, *Astrophys. J.* **341**, 1097.
Antia, H. M., Chitre, S. M., and Narasimha, D.: 1983, *Monthly Notices Roy. Astron. Soc.* **204**, 865.
Antia, H. M., Chitre, S. M., and Narasimha, D.: 1984, *Astrophys. J.* **282**, 574.
Antia, H. M., Chitre, S. M., and Pandey, S. K.: 1981, *Solar Phys.* **70**, 67.
Beckers, J. M.: 1968, *Solar Phys.* **5**, 309.
Beckers, J. M.: 1981, in S. Jordan (ed.), *The Sun as a Star*, NASA SP-450, p. 11.
Beckers, J. M. and Canfield, R. C.: 1976, in R. Cayrel and M. Steinberg (eds.), *Physique des mouvements dans les atmosphères stellaires*, Colloques Internationaux du C.N.R.S., No. 250, p. 207.
Böhm, K. H.: 1963, *Astrophys. J.* **137**, 881.
Bogart, R. S. Gierasch, P. J., and Macauslan, J. M.: 1980, *Astrophys. J.* **236**, 285.
Bumba, V.: 1970, *Solar Phys.* **14**, 80.
Chan, K. L. and Sofia, S.: 1986, *Astrophys. J.* **307**, 222.
Chou, D.-Y., LaBonte, B. J., Braun, D. C., and Duvall, T. L.: 1991, *Astrophys. J.* **372**, 314.
Cox, A. N. and Tabor, J. E.: 1976, *Astrophys. J. Suppl.* **31**, 271.
Christensen-Dalsgaard, J. and Frandsen, S.: 1983, *Solar Phys.* **82**, 469.
Deubner, F.-L.: 1989, *Astron. Astrophys.* **216**, 259.
Ginet, G. P. and Simon, G. W.: 1992, *Astrophys. J.* **386**, 359.
Giovanelli, R. G.: 1980, *Solar Phys.* **67**, 211.
Gough, D. O. and Weiss, N. O.: 1976, *Monthly Notices Roy. Astron. Soc.* **176**, 589.
Hart, A. B.: 1956, *Monthly Notices Roy. Astron. Soc.* **116**, 38.
Hart, M. H.: 1973, *Astrophys. J.* **184**, 587.
Hill, F., Deubner, F.-L., Isaak, G.: 1991, in A. N. Cox, W. C. Livingston, and M. S. Matthews (eds.), *Solar Interior and Atmosphere*, University of Arizona Press, Tucson, p. 329.
Howard, R.: 1971, *Solar Phys.* **16**, 21.
Howard, R. and LaBonte, B. J.: 1980, *Astrophys. J.* **239**, 738.
Musman, S. and Rust, D. M.: 1970, *Solar Phys.* **13**, 261.
Narasimha, D. and Antia, H. M.: 1982, *Astrophys. J.* **262**, 358.
November, L. J. and Simon, G. W.: 1988, *Astrophys. J.* **333**, 427.
November, L. J., Toomre, J., Gebbie, K. B., and Simon, G. W.: 1981, *Astrophys. J.* **245**, L123.
Roudier, T., Muller, R., Mein, P., Vigneau, J., Malherbe, J. M., and Espagnet, O.: 1991, *Astron. Astrophys.* **248**, 245.
Schröter, E. H.: 1985, *Solar Phys.* **100**, 141.
Shaviv, G. and Chitre, S. M.: 1968, *Monthly Notices Roy. Astron. Soc.* **140**, 61.
Simon, G. W. and Leighton, R. B.: 1964, *Astrophys. J.* **140**, 1120.
Simon, G. W. and Weiss, N. O.: 1968, *Z. Astrophys.* **69**, 435.
Stein, R. F. and Nordlund, Å.: 1989, *Astrophys. J.* **342**, L95.

Title, A. M., Tarbell, T. D., Simon, G. W. and the SOUP Team: 1986, *Adv. Space Res.* **6**, No. 8, 253.
Unno, W. and Spiegel, E. A.: 1966, *Publ. Astron. Soc. Japan* **18**, 85.
Vernazza, J. E., Avrett, E. H., and Loeser, R.: 1976, *Astrophys. J. Suppl.* **30**, 1.
Wang, H. and Zirin, H.: 1989, *Solar Phys.* **120**, 1.
Worden, S. P. and Simon, G. W.: 1976, *Solar Phys.* **46**, 73.
Zahn, J.-P.: 1987, in E. H. Schröter and Schüssler (eds.), *Solar and Stellar Physics*, p. 55.